ANALYSIS OF ELECTROMAGNETIC LOADS ON AN ITER DIVERTOR CASSETTE

Abstract

This paper presents essential results of transient electromagnetic (EM) analysis of International Thermonuclear Experimental Reactor (ITER) divertor cassette. The analysis is done for the ITER 2002 year reference design with the using the TYPHOON code.

Two plasma disruption scenarios fast and slow downward VDE were analysed. To optimise the use of computational resources, two independent transient EM processes were analysed separately for each scenario, and superimposed afterward. The first process associates with the Halo currents and variation of the toroidal magnetic flux generated by the plasma; and the second one caused by variations of the toroidal plasma current, shape and position.

Keywords: Electromagnetic analysis, International Thermonuclear Experimental Reactor, Divertor cassette, TYPHOON code, Downward vertical plasma displacement episode, Transient electromagnetic process, Halo current, Eddy current, Forces and moments.

Introduction

This paper presents essential results of transient electromagnetic (EM) analysis of International Thermonuclear Experimental Reactor (ITER) divertor cassette. The analysis is done for the ITER 2002 year reference design. Based on previous evaluation of electromagnetic loads, two scenarios of the plasma evolution were selected. They both begin from the downward vertical plasma displacement episode (VDE), and conclude with either fast or slow plasma disruption.

To optimise the use of computational resources, two independent transient EM processes were analysed separately for each scenario, and superimposed afterward. The first associates with the Halo currents and variation of the toroidal magnetic flux generated by the plasma; and the second caused by variations of the toroidal plasma current, shape and position.

EM loads were assessed in the following terms:

1. Distributed forces, total (integral) forces and turning moments, caused by the Halo currents and by variations of the toroidal magnetic flux;
2. Distributed forces, total (integral) forces and moments, caused by variations of the toroidal plasma current;
3. Total EM loads obtained as a superposition of two above: the loads caused by Halo currents and loads produced by variation of the toroidal plasma current.

The analysis was performed with the TYPHOON code developed in the Efremov Institute [1] (The code is described at our website: *http://www.niiefa.spb.su/res/stc/syntez/labs/nivo/prg/ typhoon/typh_e.html*). The TYPHOON code is dedicated to numerical simulation of eddy currents in interconnected thin conducting shells. Multiple inter-connections and branching of the shells helps to simulate complicated structures. The code uses a finite element representation in an integro-differential formulation in terms of a vector electric potential referred as the T-Ω method [2],[3],[4] With this method, the mesh should cover the only conducting domains, and doesn't need to cover non-conductive domains. Discretization of the initial integro-differential equation yields a dense matrix that involves extensive computational efforts and somewhat restricts the method's applicability.

1. Calculation model

A single FE model in a thin shell approximation has been employed to calculate all listed EM loads. The shells are triangulated via simplex-elements as shown in Figure 1. Due to the cyclic symmetry, the model is limited to a 1/54 of the ITER machine. It describes the double-walled vacuum vessel, a divertor cassette, the plasma, poloidal and toroidal field coils. Additional virtual elements were added to simulate the Halo current path closed through the plasma periphery. Currents in these virtual elements are assumed to vary in compliance with prescribed Halo currents.

Modeling of conducting structures

The vacuum vessel (VV) is modelled by two thin shells missing mutual electrical contact. The divertor model is shown in Figure 2. It describes the cassette body and plasma-facing components, namely the dome with reflector plates, inner and outer vertical targets [5].

The plasma-facing components are modelled in fine details so that to closely describe the actual design. There are stainless steel supports, fasteners, and poloidally elongated bronze monoblocks with internal cooling channels, covering the plasma-facing surfaces. The poloidal elements are separated in the toroidal direction with gaps to restrict the eddy currents as possible, and this is reflected in the EM model. By other words, the model reflects electrical anisotropy of the plasma-facing components, with relatively higher conductivity in the poloidal direction.

Modelling of PF and TF coils

The calculating model represents 6 CS sections, 6 PF coils and 18 D-shaped TF coils. Geometrical parameters of the coils are taken from [5].

Amere-turns of each TF coils are **9.128MA**. This corresponds to the toroidal field **5.3T** at **R=6.2m**. A toroidal field is co-directional with the toroidal plasma current, that means clockwise relative the machine's vertical axis as viewed from the above. Input graphs for the CS and PF coil currents at both scenarios were specified by the ITER Joint Central Team (JCT).

Modelling of the plasma behaviour

The plasma is represented by ~800 elementary current loops with independently varied currents, provided by JCT as input data. The toroidal plasma current flows clockwise relative the machine's vertical axis, that means co-directed with the toroidal field.

A toroidal magnetic flux generated by the plasma current is simulated with the use of a virtual toroidal solenoid located in the middle of the vacuum vessel. The solenoid generates a toroidal magnetic flux, that is a sum of a pure diamagnetic flux and a pure paramagnetic flux. The paramagnetic flux is co directional with the main toroidal field while the diamagnetic flux is opposite. In typical operating modes, paramagnetic flux dominates and dictates the direction of a resultant magnetic flux, i.e. clockwise relative the machine's vertical axis. The diamagnetic flux drops to zero at the end of the thermal quench, and the paramagnetic flux disappears at the end of plasma current quench.

Evolutions of the toroidal magnetic flux and toroidal plasma current at the fast/slow downward VDE are taken as specified by the ITER Joint Central Team.

Locations of the inlet and outlet areas for the Halo current are designated near supports of the blanket modules # 1 and #17, respectively (ref. Figure 1). Time variations of the Halo currents are prescribed by the JCT. Peak Halo currents is **4.9MA** for the fast scenario and **6.9MA** for the slow one.

2. Results

Two plasma evolution scenarios, the fast and slow ones, have been analysed for the critical loading conditions. For each one scenario two separate numeric problems were solved with different boundary conditions. These two gave currents pattern (1) caused by Halo currents and variation of the toroidal magnetic flux; and (2) caused by variations of the toroidal plasma current.

A mirror symmetry of the divertor cassette (see. Figures 1 and 2) yields a symmetrical pattern of eddy currents about the plane X_{tor}=0.

Halo currents and eddy currents associated with variations of the toroidal magnetic flux have a zero normal component of a current density vector in the plane X_{tor}=0. Density of eddy currents generated by variations of the toroidal plasma current are zero in the plane X_{tor}=0 in the tangent direction.

Consequently eddy current distributions can be calculated for a ½ of the cassette and then reflected to another half-cassette in conformity with the symmetry/antisymmetry laws. This approach allows a 50% decrease of a FE mesh size.

The total current density vector $\vec{j}_{tot}$ for each simplex element is found as $\vec{j}_{tot} = \vec{j}_1 + \vec{j}_2$, where $\vec{j}_1$ is the total density of Halo currents and eddy currents generated by a variable toroidal magnetic flux, $\vec{j}_2$ is the density of eddy currents due to variations of the toroidal plasma current.

The total force density $\vec{f}_{tot}$ acting on a simplex-element is dictated by an intercoupling of fields and generated eddy currents and expressed as

$$\vec{f}_{tot} = k \cdot \vec{f}_1 + \vec{f}_2 + \left[\vec{j}_1 \times \vec{B}_2\right] + \left[\vec{j}_2 \times \vec{B}_1\right],$$

where

$\vec{j}_1$ is the total density of Halo currents and eddy currents generated by a variable toroidal magnetic flux, $\vec{j}_1 = const$ for each simplex-element;

$\vec{j}_2$ is the density of eddy currents due to variations of the toroidal plasma current, $\vec{j}_2 = const$ for each simplex-element.

$\vec{B}_1$ is the average field per simplex-element from Halo currents and eddy currents generated by a variable toroidal magnetic flux;

$\vec{B}_2$ is the average field per simplex-element from eddy currents due to variations of the toroidal plasma current;

$\vec{B}_{ext}$ $\vec{B}_2$ is the average field per simplex-element from the plasma current, and PF and TF coil currents;

$\vec{f}_1 = \left[\vec{j}_1 \times \left(\vec{B}_1 + \vec{B}_{ext}\right)\right]$ is the force density due to Halo currents and a variable toroidal magnetic flux, $\vec{f}_1 = const$ for each simplex-element;

$\vec{f}_2 = \left[\vec{j}_2 \times \left(\vec{B}_2 + \vec{B}_{ext}\right)\right]$ is the force density due to with variations of the toroidal plasma current, $\vec{f}_2 = const$ for each simplex-element;

k is the toroidal peaking factor. $k = 1.07$ at the fast downward VDE and $k = 1.27$ at the slow downward VDE.

This approach was applied to calculate distributions of eddy currents, EM forces and joule heat load on the cassette components and assess peak integral EM forces and moments.

A dedicated code NFORCE [6] was used to transfer the distributed force density into equivalent forces concentrated at the nodes of the FE mesh The output nodal loads were used for static and dynamic structural analyses.

NFORCE code was developed at the Efremov Inst. to transform distributed values of arbitrary physical nature into nodal equivalents associated with a FE mesh. The outputs are available in different formats including the ANSYS format suitable for stress-strain computations. NFORCE is primarily aimed to solving coupled problems in variational finite-element approximation to ensure sufficiently accurate calculations. Also NFORCE is applicable for data translation among different codes.

EM loads at slow downward VDE

The operating scenario of the slow downward VDE is typically subdivided into 3 phases:

- slow vertical plasma drift;
- plasma thermal quench;
- plasma current disruption.

The slow drift phase lasts **411мс**. During this phase the plasma current centroid moves **1.5** m vertically downward. The initial plasma current and toroidal magnetic flux decrease by **11–17%,** from **15MA** and **1.14Wb** to **13.4MA** and **0.95Wb**, respectively.

The slow plasma drift is followed by a **3ms** long thermal quench. The plasma current centroid keeps moving downward, the plasma current rises to **15.7MA** and the toroidal magnetic flux peaks to **2.43Wb**.

Plasma current disruption takes place after the thermal quench, and the peak plasma current and toroidal magnetic flux fall to zero at the time mark **216ms**. The plasma downward displacement continues during the current quench.

A Halo current is practically zero during the first stage. It grows up to **6.9MA** during the thermal quench and disappears at the end of the current quench.

Figure 3 illustrates evolutions of the plasma current position, full toroidal plasma current, toroidal magnetic flux, and Halo current.

Time variations of the poloidal eddy currents are shown in Figure 4. The poloidal currents in the cassette are caused by variations of the toroidal magnetic flux and by Halo current. Peak poloidal eddy currents are in Table 1. The peak value of total poloidal current in the divertor cassette is **76.3kA**. It is about **60%** of the total Halo current, flowing in a 1/54 part of the ITER machine at **510ms**.

The total EM loads (forces and moments), acting on the divertor cassette at the slow downward VDE are shown in Figures 5 and 6. These loads have been calculated as sum of two components:

(a) EM loads due to the Halo current and a variations of the toroidal magnetic flux;

(b) EM loads due to variations of the toroidal plasma current, shape and position.

Peak EM forces and moments acting on the divertor cassette at the slow downward VDE are summarized in Table 2.

The conclusions for this scenario are the following:

- total radial and vertical EM forces acting on the divertor cassette are caused mostly by the Halo current and in a lesser degree by eddy currents associated with a variations of the toroidal magnetic flux;
- total radial and vertical moments are caused mostly by variations of the toroidal plasma current, shape and position.

EM loads at fast downward VDE

Similarly to the slow downward VDE, the operating scenario of the fast downward VDE is comprises 3 phases:

- slow vertical plasma drift;
- plasma thermal quench;
- plasma current disruption.

The plasma behaviour during the first and the second phases is similar to the previous scenario. The main difference between the slow and fast downward VDE is in values of the peak Halo current and duration of the plasma current quench. At the fast downward VDE the peak Halo current is **4.9MA**, and the current quench lasts **27ms**, in comparison to **6.9MA** and **216ms** at the slow downward VDE. Because of this, EM loads due to the Halo current and variation of the toroidal magnetic flux are expected to be smaller then before. Respectively, EM loads associated with variations of the toroidal plasma current are expected to be higher then before.

Evolutions of the plasma current position, full toroidal plasma current, toroidal magnetic flux, and Halo current at the fast downward VDE are shown in Figure 7. Figure 8 presents time variations of the poloidal eddy currents. The peak values of poloidal currents are listed in Table 3. The maximum value **68.5kA** of total poloidal current in the divertor cassette is reached at time moment **429ms**. It is about **75%** of the total Halo current in a 1/54 of the ITER machine at this time moment (**429ms**).

Figures 9 and 10 illustrate total EM loads (forces and moments) acting on the divertor components at the fast downward VDE. The total loads are calculated as sum of following components:

(a) EM loads due to the Halo current and a variable toroidal magnetic flux;
(b) EM loads due to variations of the toroidal plasma current, shape and position.

As for the slow downward VDE, the Halo current and a variable toroidal magnetic flux are predicted to produce the highest integral radial and vertical forces acting on the divertor components. Integral radial and vertical moments are dictated by a rate of a toroidal plasma current variation. Peak values of EM forces and moments at the fast downward VDE are summarized in Table 4.

A comparison of EM loads obtained for both scenarios suggests that the maximal radial and vertical EM forces of, respectively, **-837kN** and **-1.89MN** would occur at the slow downward VDE at the peak Halo current. The maximal radial moment of **-1.11MN·m** and vertical moment of **-4.38MN·m** are expected to take place at the fast downward VDE at the end of the current disruption. The stress analysis performed on the basis of the obtained distributed EM loads have demonstrated that the fast downward VDE would produce the most crucial loading conditions. A numerical simulation predicts unacceptable mechanical overloads on the fasteners of the vertical targets and the dome [7].

To reduce EM loads an electrical gap may be arranged at the symmetry plane of the cassette. The gap would prevent the loops of eddy currents generated by the toroidal plasma current variations from closing that should diminish EM loads.

Conclusions

- A dominant portion of total EM forces, radial and vertical, applied to the ITER divertor cassette during the downward VDE is one associated with Halo currents and variations of the toroidal magnetic flux.
- A dominant portion of total EM moments, radial and vertical, is one caused by variations of the toroidal plasma current.
- As for slow downward VDE, the maximal radial and vertical EM forces are reached at the time when the Halo current peaks (**6.9MA)**. The maximum radial force is **-837kN** and the vertical one is **-1.89MN**.
- The maximal radial moment of **-1.11MN·m** and the vertical one of **-4.38MN·m** are expected at the fast downward VDE at the end of the current disruption when the highest rate of the plasma current decrease of **–1107MA/s** occurs.
- The stress analysis performed on the basis of the calculated EM loads predicts mechanical overloading on the fasteners of the vertical targets and the dome at the fast downward VDE.
- A modification in the design of the vertical targets and the dome is recommended to reduce the loads. An electrical gap is proposed at the symmetry plane of the cassette

to cut the loops of eddy current generated by the toroidal plasma current variations and consequently lower EM loads on these components.

References

[1] A.V.Belov, N.I.Doinikov, A.E.Duke, V.V.Kokotkov, M.D.Korolkov, V.L.Kotov, V.P.Kukhtin, E.A.Lamzin, S.E.Sytchevsky: “Transient electromagnetic analysis in tokamaks using TYPHOON code”, Fusion Engineering and design 31 (1996), p167-180.

[2] Preston T.W., Reece A.B.J. “Solution of 3D eddy current problems: T-Ω method”, IEEE Trans. Mag., Vol.18, N2, March 1982, p.486.

[3] Albanese R., Martone R., Miano G., Rubinacci G.: “Formulation for 3D finite-element eddy current computation”, IEEE Trans. Mag., Vol.21, N6, Nov. 1985, p.2299.

[4] Makata T., Takahashi N., Fujiwara K., Okada Y, “Improvements of the T-Ω method for 3D eddy current analysis”, IEEE Trans. Mag. Vol.24, N1, Jan. 1988, p.94.

[5] ITER Technical Basis, ITER EDA Documentation Series No.24, IAEA, Vienna, 2002.

[6] A.Alekseev, A.Arneman, A.Belov, T.Belyakova, L.Chvartatskaya, O.Filatov, V.Kokotkov, V.Kukhtin, E.Lamzin, A.Malkov, N.Shatil, S.Sytchevsky: “On the calculation of concentrated loads at finite-element mesh nodes as equivalents of a given spatial distribution of volume force density”, Plasma Devices and Operations, 2002, Vol. 10(4), pp. 269-284.

[7] N.Berkhov, V.Komarov, A.Labusov, I.Labusov, A.Malkov, “Dynamic Analysis of ITER Divertor Cassette under EM loads”, Plasma Devices and Operations, 12, No.1, 11-17 (2004).

Table 1: Currents induced in divertor components by Halo currents and variations of toroidal magnetic flux at the slow downward VDE: predictions for the maximum currents and currents at 513ms, when a peak Halo current occurs.

Divertor Components	Peak current, (kA)	Current at 513ms, (kA)
From VV to CB	76.31 (510ms)	75.47 (513ms)
In lower part of VV (under divertor)*	32.52 (549ms)	29.89 (513ms)
In upper part of VV*	30.02 (414ms)	23.69 (513ms)
From CB to Inner VT	24.51 (459ms)	18.90 (513ms)
From CB to Dome	56.79 (483ms)	51.43 (513ms)
From CB to Outer VT	33.59 (459ms)	24.24 (513ms)

(*)the total poloidal current flowing in 1/54 part of VV.

Table 2: The maximum values of the total EM loads at the slow downward VDE. The loads are given in a local coordinate system (see Figure 1) and presented as a) radial, b) toroidal and c) vertical forces and values of d) radial, e) toroidal and f) vertical moments.

Divertor Components	F_{rad} (kN)	F_{tor} (kN)	F_{ver} (kN)	M_{rad} (kN·m)	M_{tor} (kN·m)	M_{ver} (kN·m)
Inner VT	-139 (414ms)	36.8 (579ms)	44.4 (459ms)	441 (414ms)	-104 (414ms)	-178 (579ms)
Outer VT	248 (459ms)	103 (579ms)	-147 (414ms)	-285 (414ms)	-191 (414ms)	-481 (579ms)
Dome with reflector plates	-257 (483ms)	-142 (414ms)	-647 (483ms)	360 (414ms)	-24.3 (414ms)	700 (414ms)
Cassette body	-708 (528ms)	-205 (414ms)	-1320 (531ms)	-268 (419ms)	182 (510ms)	-985 (579ms)
Whole divertor cassette	-837 (528ms)	-440 (414ms)	-1890 (510ms)	-582 (579ms)	198 (495ms)	-2070 (579ms)

Table 3: Currents induced in divertor components by Halo currents and variations of toroidal magnetic flux at the fast downward VDE: predictions for the maximum currents and currents at 426ms, when a peak Halo current occurs.

Divertor Components	Peak current, (kA)	Current at 426ms, (kA)
From VV to CB	68.46 (429ms)	66.97 (426ms)
In lower part of VV (under divertor)*	12.85 (435ms)	9.75 (426ms)
In upper part of VV*	30.11 (414ms)	16.22 (426ms)
From CB to Inner VT	42.02 (426ms)	42.02 (426ms)
From CB to Dome	66.78 (429ms)	65.77 (426ms)
From CB to Outer VT	51.43 (426ms)	51.43 (426ms)

(*) the total poloidal current flowing in 1/54 part of VV.

Table 4: The maximum values of the total EM loads at the fast downward VDE. The loads are given in a local coordinate system (see Figure 1) and presented as a) radial, b) toroidal and c) vertical forces and values of d) radial, e) toroidal and f) vertical moments.

Divertor Components	F_{rad} (kN)	F_{tor} (kN)	F_{ver} (kN)	M_{rad} (kN·m)	M_{tor} (kN·m)	M_{ver} (kN·m)
Inner VT	-188 (423ms)	59.5 (435ms)	-83.5 (441ms)	-754 (438ms)	-102 (417ms)	-283 (435ms)
Outer VT	311 (423ms)	220 (438ms)	-159 (417ms)	-285 (414ms)	205 (417ms)	-1050 (438ms)
Dome with reflector plates	-252 (429ms)	209 (438ms)	-644 (426ms)	-559 (438ms)	27.1 (438ms)	-989 (438ms)
Cassette body	-446 (426ms)	395 (438ms)	-786 (429ms)	495 (442ms)	235 (438ms)	-1930 (438ms)
Whole divertor cassette	-515 (429ms)	913 (438ms)	-1400 (426ms)	-1110 (438ms)	261 (438ms)	-4380 (438ms)

FIGURE CAPTIONS

Figure 1: Finite element model of a 1/54 part of the ITER machine. The global Cartesian coordinate system (X_{rad}; X_{tor}; X_{ver}) with the origin at the machine centre.

Figure 2: Finite element model of an ITER divertor cassette. A local Cartesian coordinate system. The axes of the local coordinate system are directed the same way as the axes of the global coordinate system (see Figure 1). The origin of the local system is positioned as (4.818; 0.0; -4.1001) in the radial, toroidal and vertical coordinates of the global system.

Figure 3: Evolutions of plasma parameters during the slow downward VDE. "I_{tor}" – full toroidal plasma current, "I_{halo}" – poloidal component of Halo current, "Φ" – toroidal magnetic flux associated with plasma current, "R" and "Z" indicate the radial and vertical displacements of the plasma centroid.

Figure 4: Evolutions of currents induced in divertor components by the Halo current and variations of a toroidal magnetic flux during the slow downward VDE.

- solid line - current flowing in 1/54 part of machine;
- diamond-marked line - current flowing from the VV to the divertor cassette;
- cross-marked line - current flowing from the cassette body to the private flux region components;
- circle-marked line - current flowing from the cassette body to the outer vertical target;
- box-marked line - current flowing from the cassette body to the inner vertical target;
- triangle-marked line - poloidal current flowing under divertor cassette in a 1/54 lower part of the VV.

Figure 5: Evolution of the <u>total</u> forces applied to the <u>whole divertor cassette</u> during the slow downward VDE. The forces are given in the local coordinate system (see Figure 2).

Figure 6: Evolution of the <u>total</u> torque moments applied to the <u>whole divertor cassette</u> during the slow downward VDE. The moments are given in the local coordinate system (see Figure 2).

Figure 7: Evolutions of plasma parameters during the fast downward VDE. "I_{tor}" – full toroidal plasma current, "I_{halo}" – poloidal component of Halo current, "Φ" – toroidal magnetic flux associated with plasma current, "R" and "Z" indicate the radial and vertical displacements of the plasma centroid.

Figure 8: Evolutions of currents flowing through divertor components and caused by Halo current and variation of the toroidal magnetic flux during fast downward VDE.

- solid line - Halo current flowing in 1/54 part of machine;
- diamond-marked line - current flowing from the VV to the divertor cassette;
- cross-marked line - current flowing from the cassette body to the private flux region components;
- circle-marked line - current flowing from the cassette body to the outer vertical target;
- box-marked line - current flowing from the cassette body to the inner vertical target;
- triangle-marked line - poloidal current flowing under divertor cassette in a 1/54 lower part of the VV.

Figure 9: Evolution of the total forces applied to the whole divertor cassette during the fast downward VDE. The forces are given in the local coordinate system (see Figure 2).

Figure 10: Evolution of the total torque moments applied to the whole divertor cassette during the fast downward VDE. The moments are given in the local coordinate system (see Figure 2).

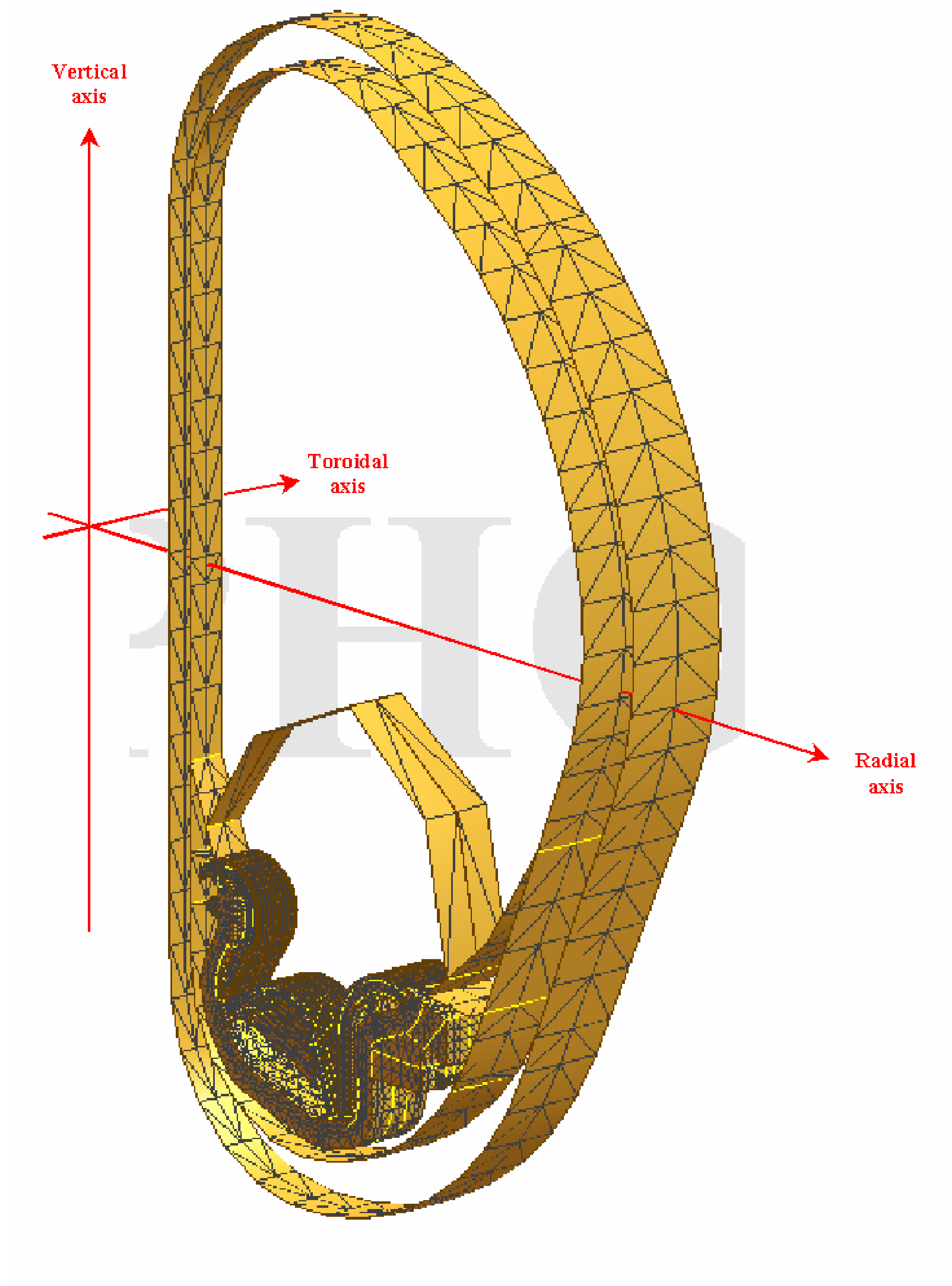

Figure 1

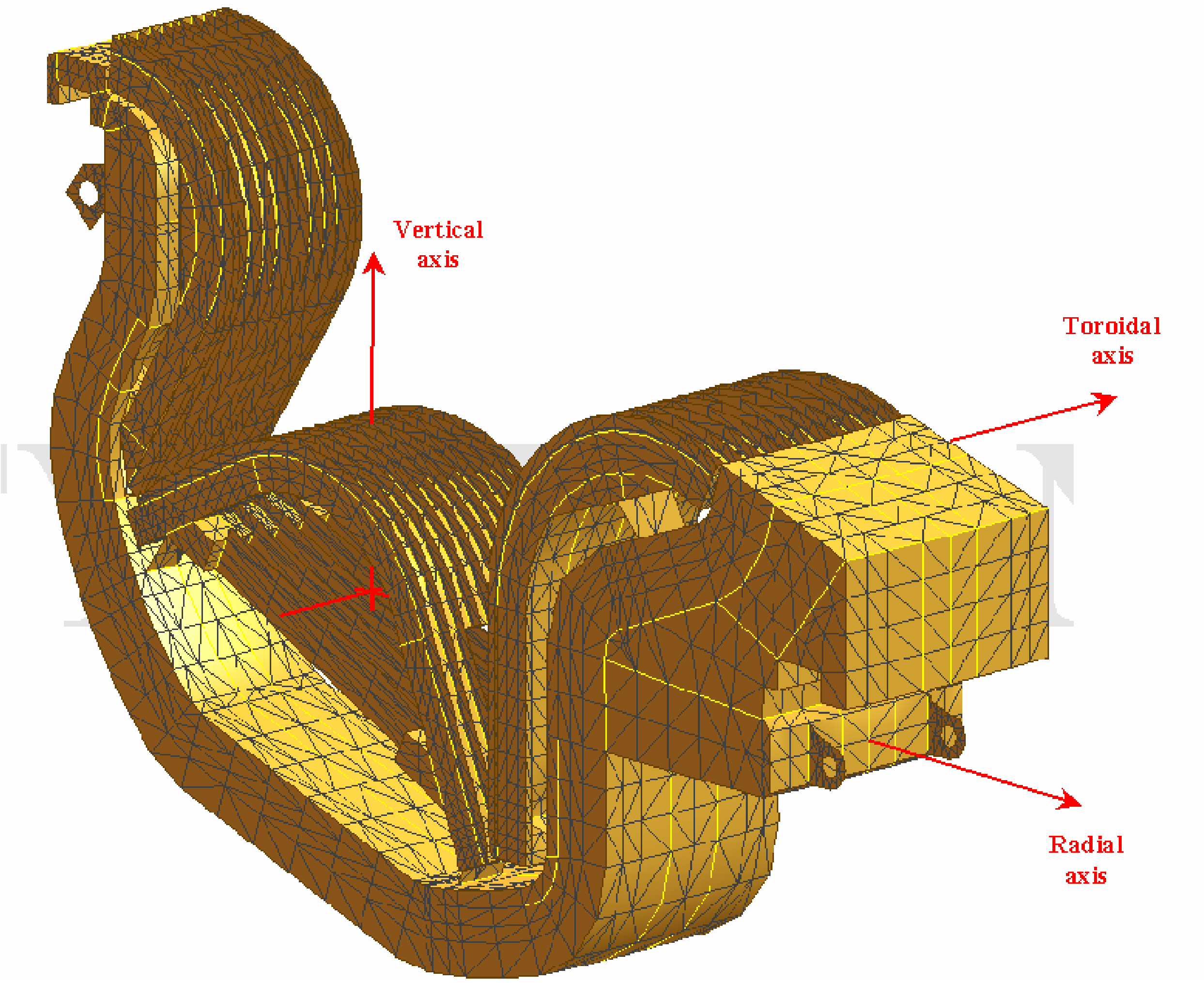

Figure 2

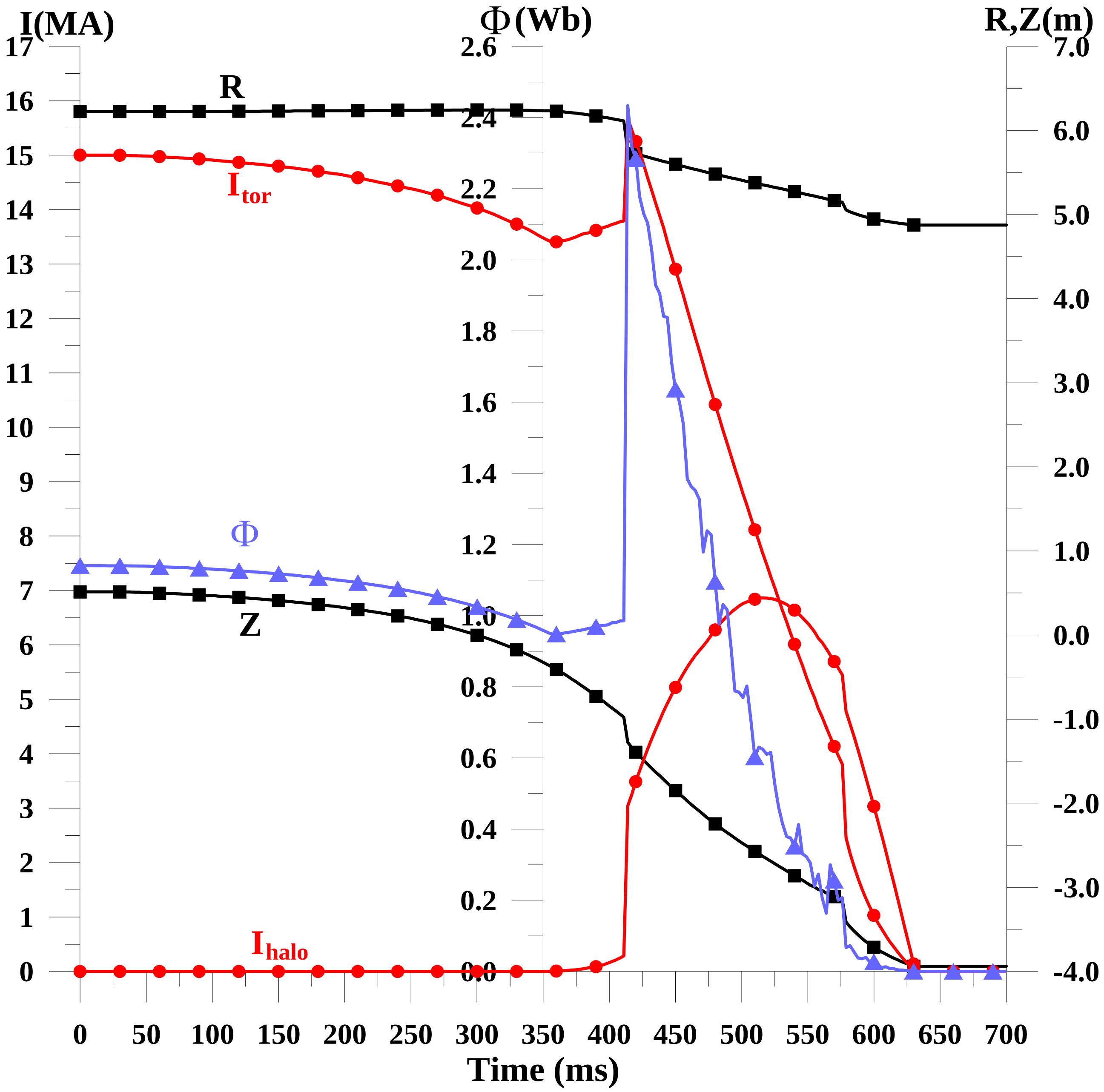
I(MA)
Φ(Wb)
R,Z(m)
R
Itor
Φ
Z
Ihalo
17
16
15
14
13
12
11
10
9
8
7
6
5
4
3
2
1
0
2.6
2.4
2.2
2.0
1.8
1.6
1.4
1.2
1.0
0.8
0.6
0.4
0.2
0.0
7.0
6.0
5.0
4.0
3.0
2.0
1.0
0.0
-1.0
-2.0
-3.0
-4.0
0
50
100
150
200
250
300
350
400
450
500
550
600
650
700
Time (ms)

Figure 3

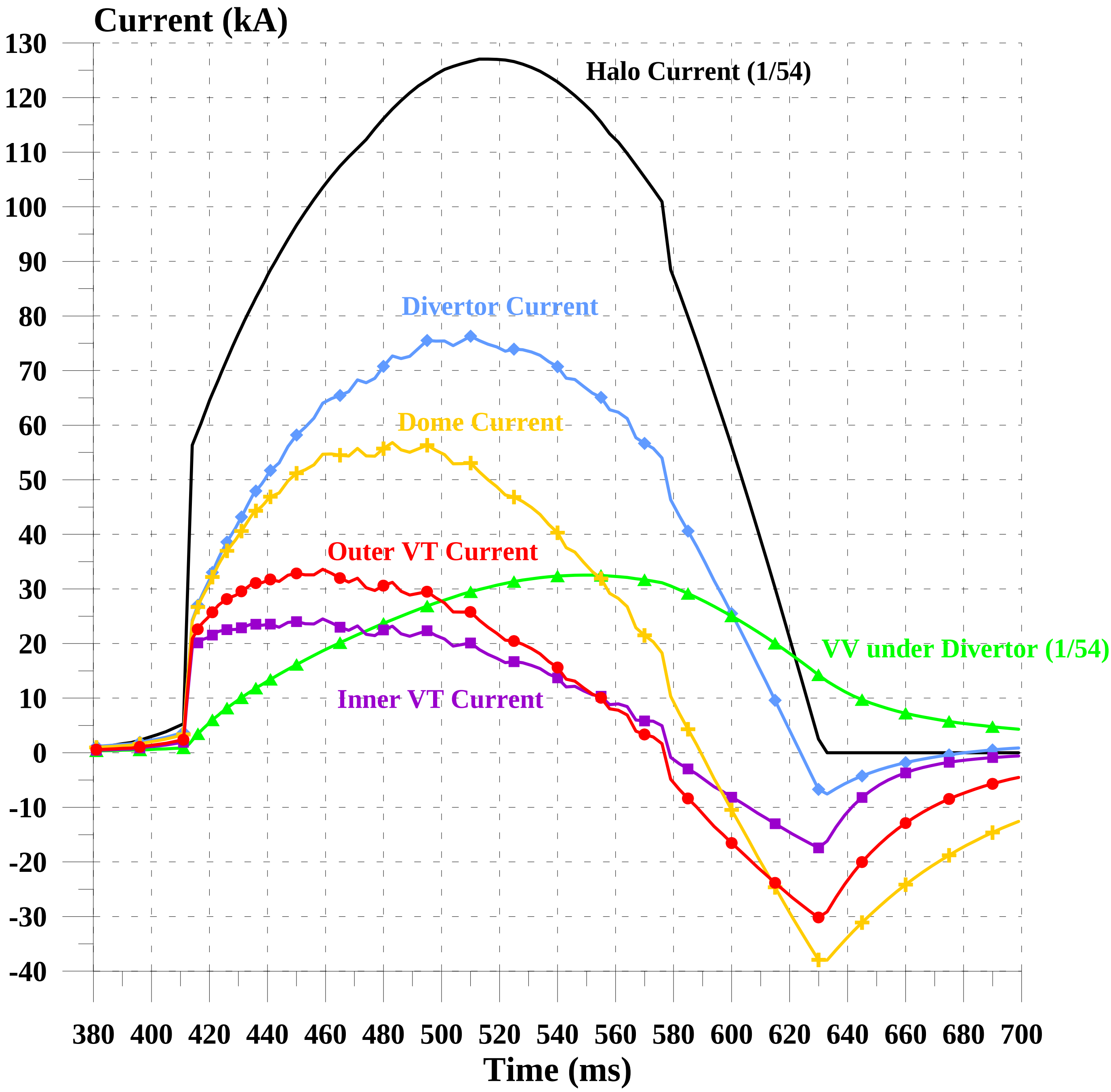
Current (kA)
130
120
110
100
90
80
70
60
50
40
30
20
10
0
-10
-20
-30
-40
Halo Current (1/54)
Divertor Current
Dome Current
Outer VT Current
VV under Divertor (1/54)
Inner VT Current
380 400 420 440 460 480 500 520 540 560 580 600 620 640 660 680 700
Time (ms)

Figure 4

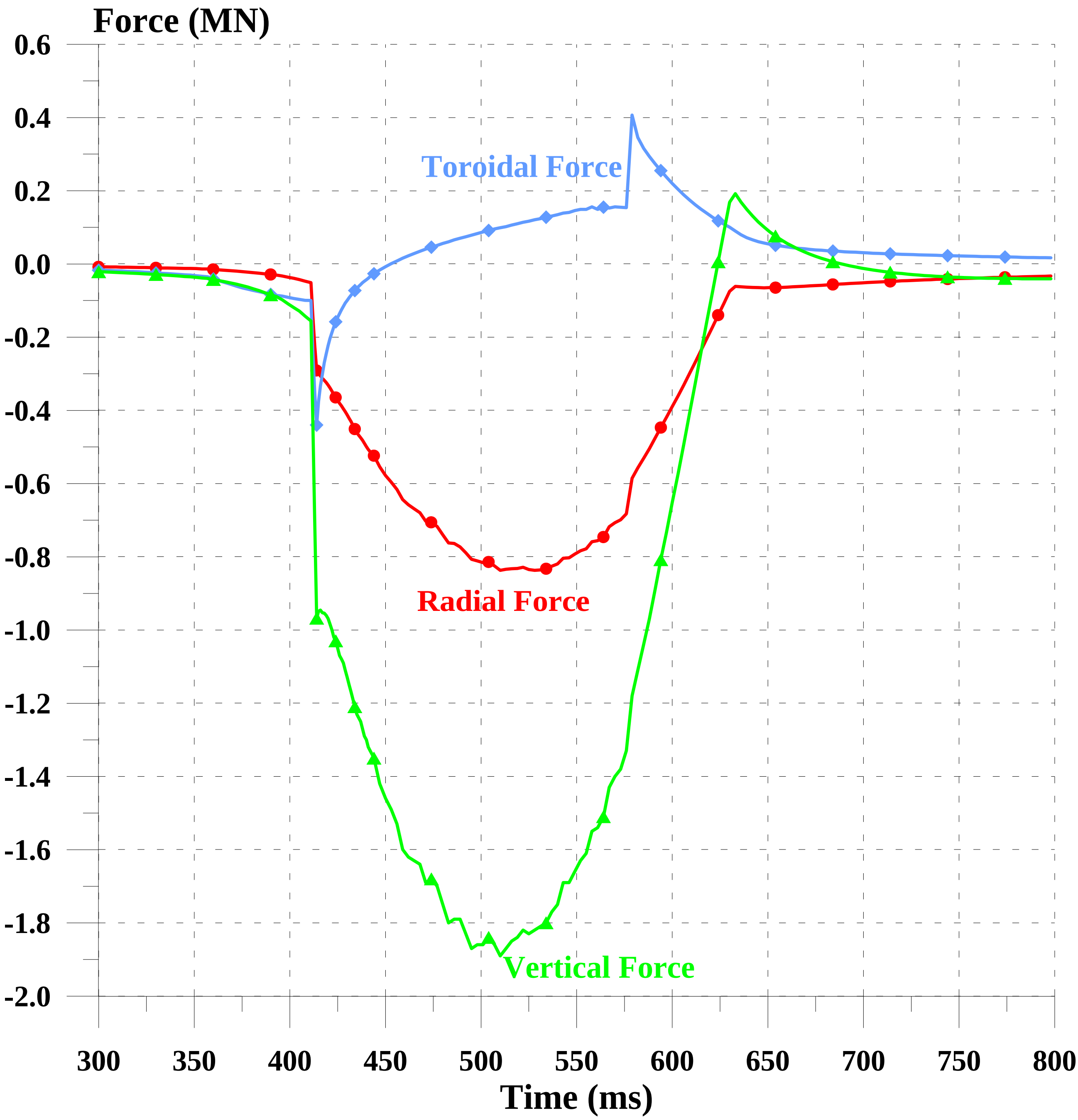
Force (MN)
0.6
0.4
0.2
0.0
-0.2
-0.4
-0.6
-0.8
-1.0
-1.2
-1.4
-1.6
-1.8
-2.0
Toroidal Force
Radial Force
Vertical Force
300
350
400
450
500
550
600
650
700
750
800
Time (ms)

Figure 5

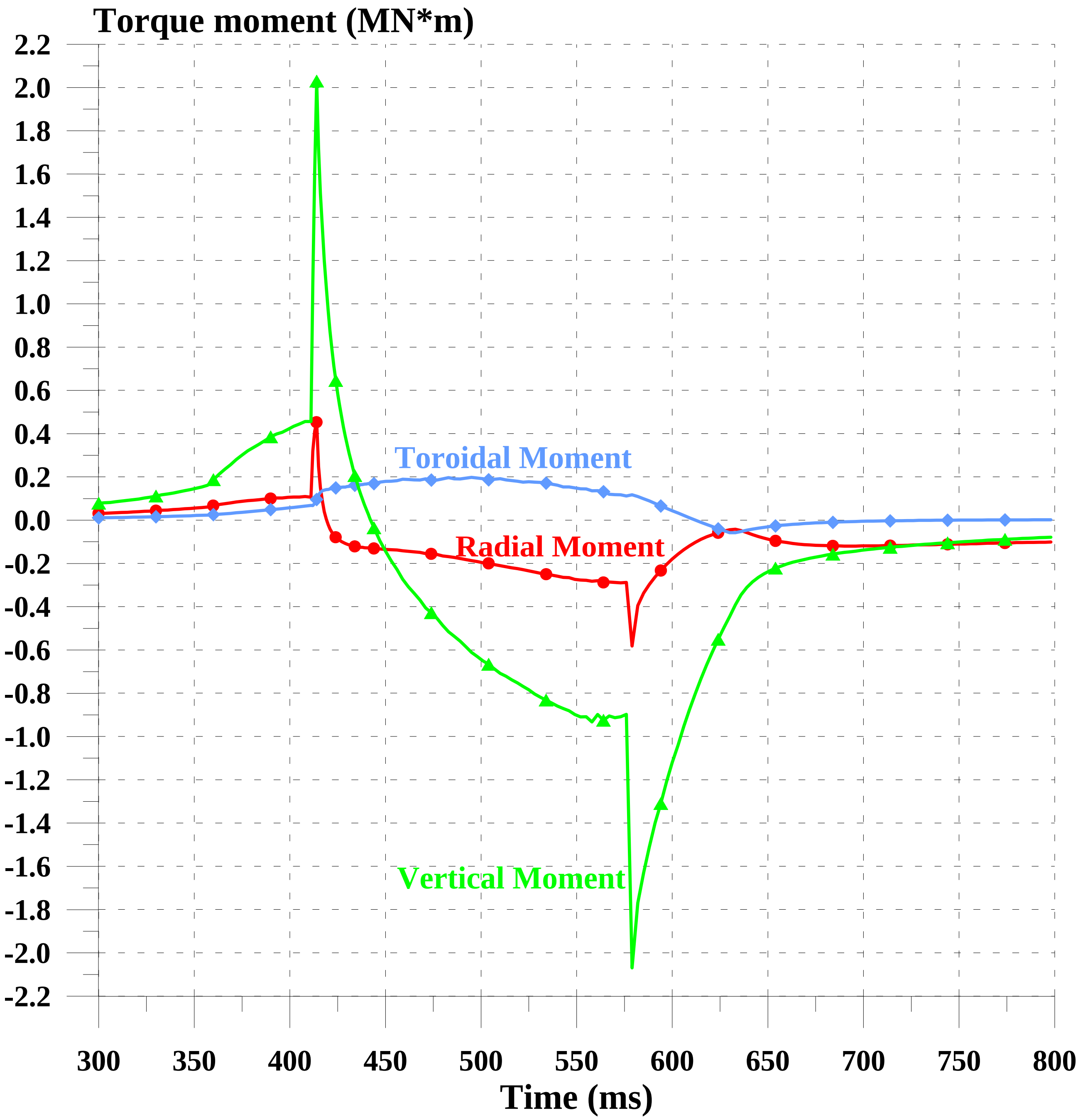
Torque moment (MN*m)
2.2
2.0
1.8
1.6
1.4
1.2
1.0
0.8
0.6
0.4
0.2
0.0
-0.2
-0.4
-0.6
-0.8
-1.0
-1.2
-1.4
-1.6
-1.8
-2.0
-2.2
Toroidal Moment
Radial Moment
Vertical Moment
300
350
400
450
500
550
600
650
700
750
800
Time (ms)

Figure 6

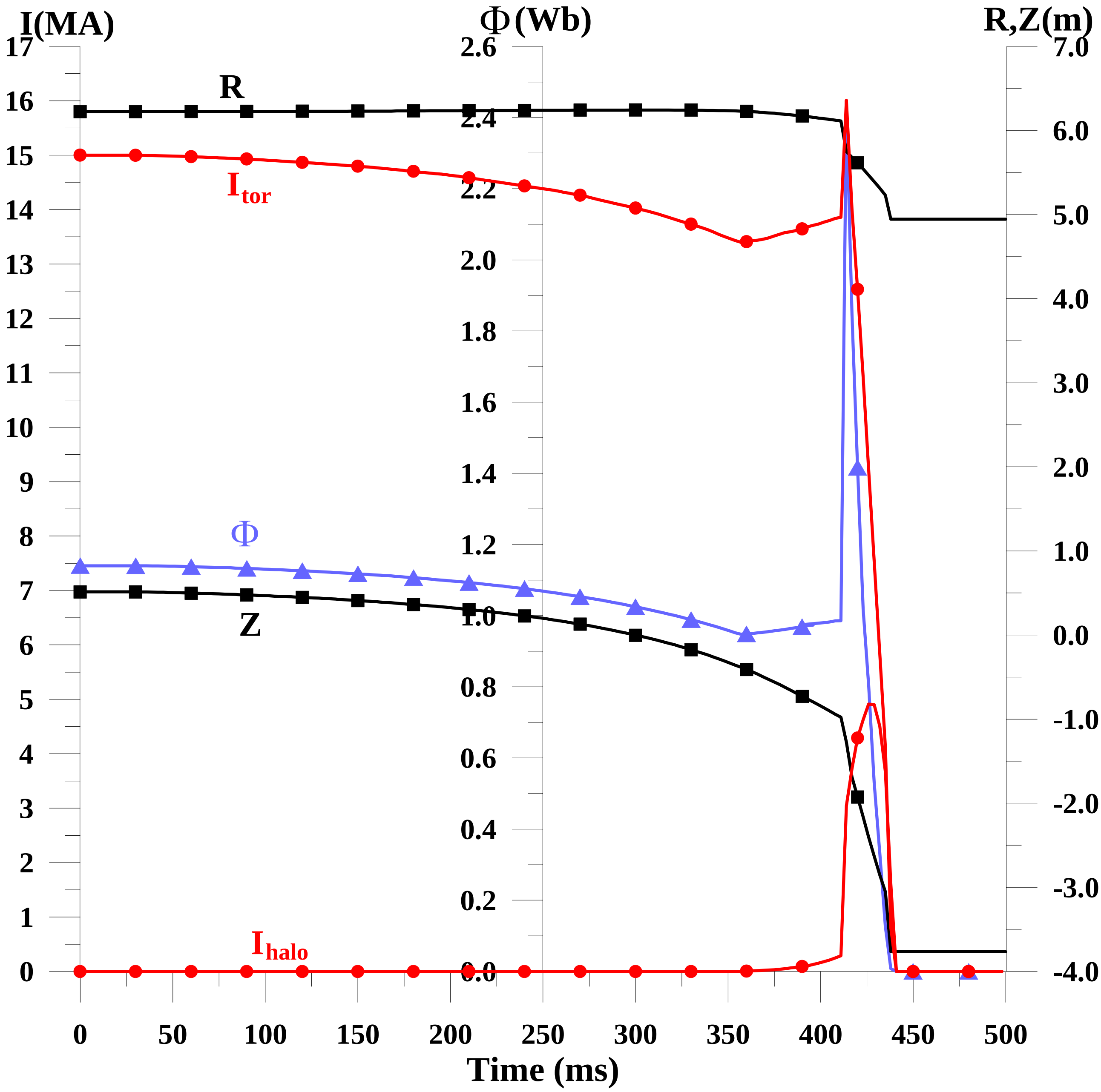
I(MA)
Φ (Wb)
R,Z(m)
R
I_tor
Φ
Z
I_halo
17
16
15
14
13
12
11
10
9
8
7
6
5
4
3
2
1
0
2.6
2.4
2.2
2.0
1.8
1.6
1.4
1.2
1.0
0.8
0.6
0.4
0.2
0.0
7.0
6.0
5.0
4.0
3.0
2.0
1.0
0.0
-1.0
-2.0
-3.0
-4.0
0
50
100
150
200
250
300
350
400
450
500
Time (ms)

Figure 7

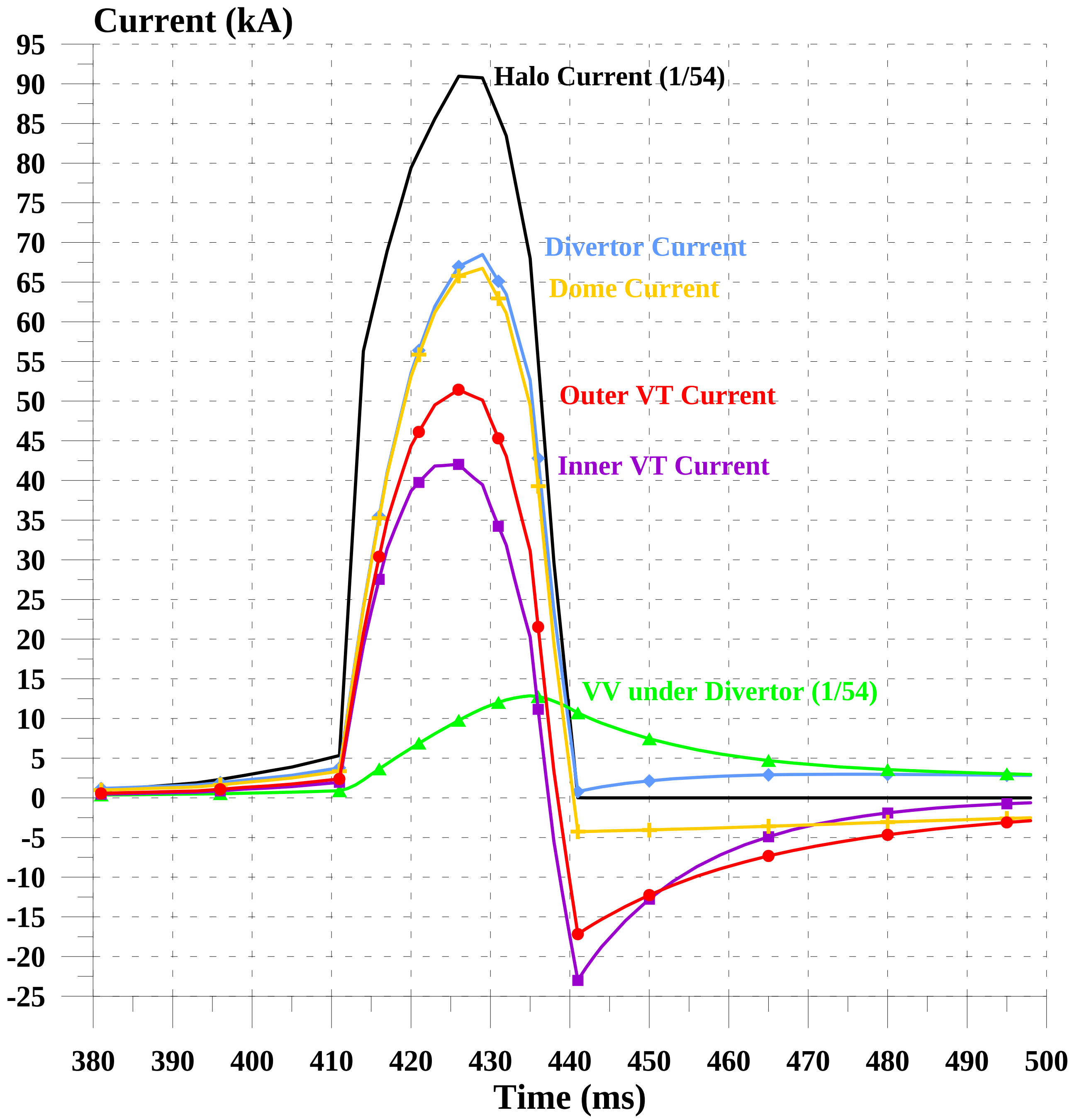
Current (kA)
95
90
85
80
75
70
65
60
55
50
45
40
35
30
25
20
15
10
5
0
-5
-10
-15
-20
-25
Halo Current (1/54)
Divertor Current
Dome Current
Outer VT Current
Inner VT Current
VV under Divertor (1/54)
380
390
400
410
420
430
440
450
460
470
480
490
500
Time (ms)

Figure 8

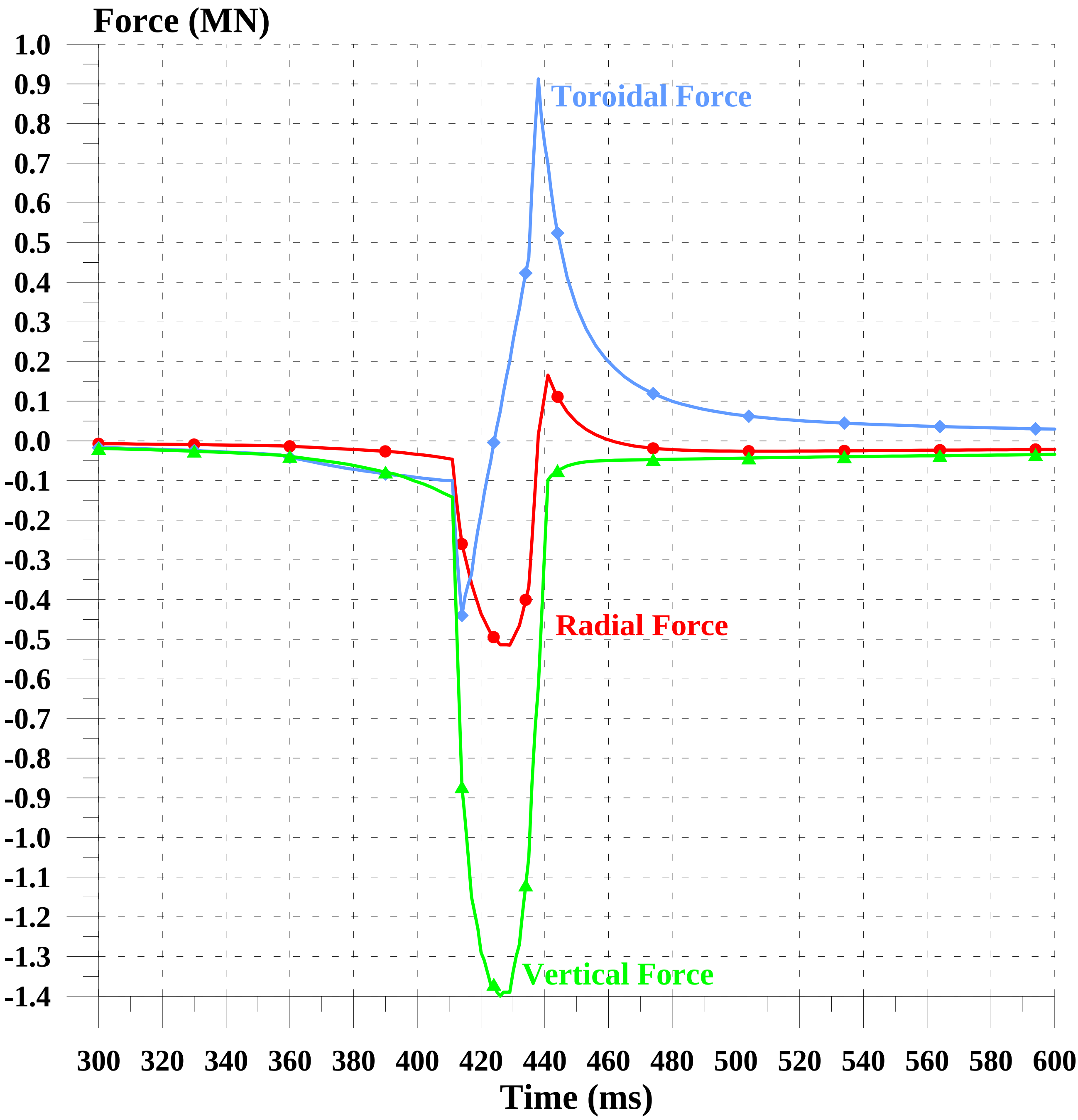
Force (MN)
1.0
0.9
0.8
0.7
0.6
0.5
0.4
0.3
0.2
0.1
0.0
-0.1
-0.2
-0.3
-0.4
-0.5
-0.6
-0.7
-0.8
-0.9
-1.0
-1.1
-1.2
-1.3
-1.4
Toroidal Force
Radial Force
Vertical Force
300
320
340
360
380
400
420
440
460
480
500
520
540
560
580
600
Time (ms)

Figure 9

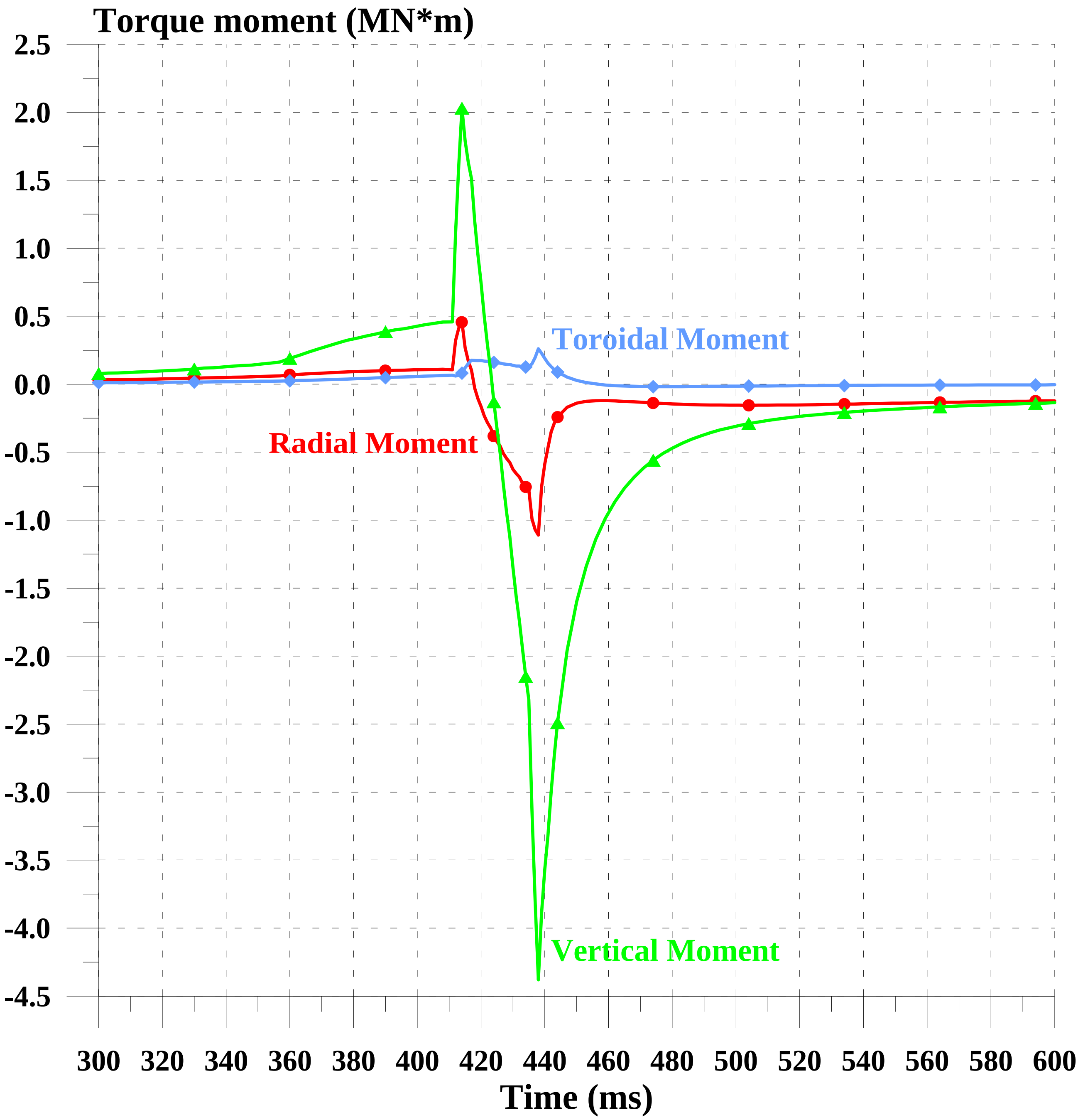
Torque moment (MN*m)
2.5
2.0
1.5
1.0
0.5
0.0
-0.5
-1.0
-1.5
-2.0
-2.5
-3.0
-3.5
-4.0
-4.5
Toroidal Moment
Radial Moment
Vertical Moment
300 320 340 360 380 400 420 440 460 480 500 520 540 560 580 600
Time (ms)

Figure 10